Journal of Micromechanics
and Microengineering

Pressure gradient and electroosmotic effects on two immiscible fluids in a microchannel between two parallel plates

To cite this article: Guyh Dituba Ngoma and Fouad Erchiqui 2006 *J. Micromech. Microeng.* **16** 83

INSTITUTE OF PHYSICS PUBLISHING JOURNAL OF MICROMECHANICS AND MICROENGINEERING

J. Micromech. Microeng. **16** (2006) 83–91 doi:10.1088/0960-1317/16/1/012

Pressure gradient and electroosmotic effects on two immiscible fluids in a microchannel between two parallel plates

Guyh Dituba Ngoma and Fouad Erchiqui

Department of Applied Sciences, University of Quebec in Abitibi-Temiscamingue, 445, Boulevard de l'Université, Rouyn-Noranda, Quebec, J9X 5E4, Canada

E-mail: guyh.dituba-ngoma@uqat.ca

Received 11 September 2005, in final form 4 November 2005
Published 13 December 2005
Online at stacks.iop.org/JMM/16/83

Abstract

A model of the flow of two immiscible fluids in a microchannel between two parallel plates was made. The concept of pumping a nonconducting fluid using interfacial viscous shear stress was applied while taking into account the combined effect of the pressure gradient and electroosmosis. To determine the electric potential and flow parameters, the Poisson–Boltzmann equation and modified Navier–Stokes equations were solved for a steady fully-developed laminar flow. The results obtained demonstrate the influence of the pressure difference, the dynamic viscosity ratio, the wall and interfacial zeta potentials, the interface location and the interfacial shear stress on the flow characteristics of both fluids. A comparison of results was performed to validate the developed approach.

Nomenclature

e elementary charge (C)
E external electric field strength (V m^{-1})
h distance between the two plates (m)
k_b Boltzmann constant (J K^{-1})
L plate length (m)
n_∞ ionic number concentration in the bulk solution (m^{-3})
p pressure (Pa)
T absolute temperature (K)
u flow velocity (m s^{-1})
u_m cross-sectional mean velocity (m s^{-1})
u_0 reference velocity (m s^{-1})
x horizontal coordinate (m)
y vertical coordinate (m)
z_0 valence of ions

Greek

α dynamic viscosity ratio
ε dimensionless dielectric constant
ε_0 permittivity of vacuum (C m^{-1} V^{-1})
ϕ electric potential (V)
κ Debye–Hückle parameter
μ viscosity (Pa s)
ρ fluid density (kg m^{-3})
ρ_e electric charge density (C m^{-3})
ζ_1 zeta potential on the bottom wall (V)
ζ_2 interfacial zeta potential (V)

Subscripts

1 fluid 1: conducting fluid
2 fluid 2: nonconducting fluid

Superscripts

$*$ dimensionless parameter
$-$ means value

1. Introduction

Nowadays, microfluidic transport plays an important role in the fields of micropower generation, chemical processes, biomechanical processes and heat transfer. The flow in microchannels can be controlled using a pressure gradient or an electric field to produce an electroosmotic flow [1]. When an electrolyte comes in contact with a microchannel wall in which the fluid flows, it will result in a charge transfer between the electrolyte and the wall, depending on the chemical composition of the microchannel and the electrolyte chemical processes at the surface. The wall and the electrolyte get

oppositely charged while maintaining global charge neutrality. The charged surface affects the electrolyte solution in two ways: it influences the distribution of nearby ions in the solution and results in the formation of a region close to the charged surface called an electric double layer (EDL). In the EDL, there is an excess of counterions over coions to neutralize the surface charge. Instead of imposing an external pressure gradient when an external electric field is applied, the fluid flow forming an electroosmotic flow is induced by the EDL. The Debye length, also called the thickness of the EDL, is dependent on the bulk ionic concentration and electric fluid properties. The EDL affects the flow for an externally applied pressure gradient by retarding the fluid flow, which results in a streaming potential. To move the fluid through microsystems, electroosmotic pumps are suitable because of the absence of moving parts and pulsating flows [2]. In electroosmotic pumps, a fluid is driven by applying an electric field to the EDL, which is formed when a fluid has a sufficiently high concentration of dissociated ions. Some fluids, such as nonpolar fluids with very low conductivity, cannot form EDLs. They cannot be pumped using electroosmotic pumps. Therefore, to move such fluids, an electroosmotic flow, which is driven through layers of conducting fluid, is used indirectly to pump a nonconducting nonpolar fluid through a microchannel by viscous forces [3]. To ensure the reliability, safety and stability of the microfluidic devices used to pump a nonconducting fluid by means of a conducting fluid, precise knowledge of the two immiscible fluids flow behavior in microchannels is very important. Its investigation has to be considered in the planning and design phases of microfluidic devices. This makes it possible to avoid critical operating conditions, which can lead to damaged microchannels. Most previous investigations of pressure gradient and electroosmotic flow in microchannels were performed using a single conducting fluid [3–7] with the zeta potentials at the microchannel walls. Mathematical models were developed for steady-state fluid flow. This experiment examined the effects of surface potential, electric field, ionic concentration and channel size on the velocity distribution and the effect of friction on flow characteristics. In addition, some previous studies were performed using two immiscible fluids under an imposed electric field or pressure gradient [8, 9]. Moreover, the analysis of previous works reveals that the results are specific to the microchannel configuration. Therefore, they cannot be extrapolated to other configurations. In this work, a mathematical model was developed to predict and analyze the flow characteristics of the two immiscible fluids in a microchannel between two plates using the principle of pumping electric nonconducting fluids by means of an electric conducting fluid in microchannels. The effect of the pressure gradient is taken into account for the flow of both fluids, whereas only the electric field was used in the majority of the previous works. The Poisson–Boltzmann equation is used for the conducting fluid and the modified Navier–Stokes equations, for a steady fully-developed laminar flow, are applied to both fluids. The obtained system of partial equations is solved analytically in order to determine the distribution of the flow velocity, the volumetric flow rate, the shear stress and the electric potential. The boundary conditions for the no-slip velocity, the interfacial velocity, the interfacial shear stress, the wall and interfacial zeta potentials are taken into account in the final obtained equations. Based on the found equations, a FORTRAN program was developed to investigate and analyze the effects of pressure, the dynamic viscosity ratio, the wall and interfacial zeta potentials, the interface location and the interfacial shear stress on the static flow behavior of the two immiscible fluids.

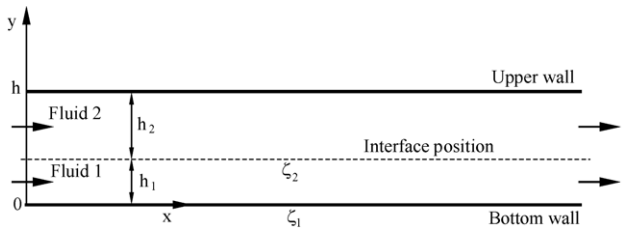

Figure 1. Two immiscible fluids in a microchannel between the two parallel plates.

2. Model description

The considered model of the two immiscible fluids flow in a microchannel between two parallel plates is shown in figure 1. The two plates are separated by a distance h. The microchannel is filled with an electric conducting fluid, fluid 1 and an electric nonconducting fluid, fluid 2. Since the fluids are different, they have different viscosities, μ_1 and μ_2, and different velocities, u_1 and u_2. The interface location is designed using the height h_1. The forces acting on an element of fluid 1 include the pressure force and the electric body force generated by the double layer electric field. For fluid 2, it is assumed that only the pressure force acts on it. To examine the system, a Cartesian orthonormal coordinate system (x, y) is used with the origin point at the bottom wall. A planar interface is assumed between the two fluids. The EDL only forms near the microchannel wall in contact with the conducting fluid and at the interface between both fluids. Thus, the zeta potential at the bottom wall is ζ_1 and that at the interface is ζ_2.

3. Governing equations

To develop the governing equations for the considered model, the following assumptions were made:

i. A steady state, one-dimensional and laminar flow was assumed.
ii. No-slip boundary conditions were assumed.
iii. A planar interface between the two immiscible fluids was assumed.
iv. The two immiscible fluids had the same velocity at the interface.
v. The shear stress and flow velocity were the same on the two fluids at the interface.
vi. The fluids were assumed to be incompressible.
vii. The gravity effect was negligible.

To account for these assumptions, the theoretical analysis of the flow of the two immiscible fluids in a microchannel, as shown in figure 1, is based on the Poisson–Boltzman equation and the modified Navier–Stokes equations.

3.1. Electric potential field

According to the electrokinetic [1], the partial differential equation of the electric potential of ions, ϕ, in y direction is given as

$$\frac{\mathrm{d}^2\phi}{\mathrm{d}y^2} = -\frac{\rho_e}{\varepsilon\varepsilon_0} \tag{1}$$

where ε is the dielectric constant of the solution, ε_0 the permittivity of vacuum and ρ_e the net charge density.

The net charge density can be written assuming a symmetric electrolyte as

$$\rho_e = -2n_\infty z_0 e \sinh\left(\frac{z_0 e}{k_b T}\phi\right) \tag{2}$$

where e, k_b, n_∞, T and z_0 are the elementary charge, Boltzmann constant, bulk concentration of ions, absolute temperature and valence of ions, respectively.

The other symbols, subscripts and superscripts used were defined in the nomenclature.

When substituting equation (2) into equation (1), equation (3) is found to be

$$\frac{\mathrm{d}^2\phi}{\mathrm{d}y^2} = \frac{2n_\infty z_0 e}{\varepsilon\varepsilon_0}\sinh\left(\frac{z_0 e}{k_b T}\phi\right). \tag{3}$$

When using the Debye–Hückel approximation,

$$\frac{2n_\infty z_0 e}{\varepsilon\varepsilon_0}\sinh\left(\frac{z_0 e}{k_b T}\phi\right) \approx \frac{2n_\infty z_0 e}{\varepsilon\varepsilon_0}\frac{z_0 e}{k_b T}\phi, \tag{4}$$

which physically means a small electric potential, in comparison with a thermal energy of ions, $|z_0 e\phi| < k_b T$, equation (3) can be written as

$$\frac{\mathrm{d}^2\phi}{\mathrm{d}y^2} = \frac{2n_\infty z_0 e}{\varepsilon\varepsilon_0}\left(\frac{z_0 e}{k_b T}\phi\right). \tag{5}$$

After transforming equation (5), it becomes

$$\frac{\mathrm{d}^2\phi}{\mathrm{d}y^2} = \kappa^2\phi \tag{6}$$

where $\kappa = z_0 e\sqrt{\frac{2n_\infty}{\varepsilon\varepsilon_0 k_b T}}$ is the Debye–Hückel parameter and $\frac{1}{\kappa}$ is the Debye length.

When the Debye–Hückel approximation in equation (2) is taken into account, it can be written as

$$\rho_e = 2n_\infty z_0 e\left(-\frac{z_0 e}{k_b T}\phi\right). \tag{7}$$

After arranging equation (7), it can be expressed as

$$\rho_e = \frac{-2n_\infty z_0^2 e^2\phi}{k_b T}. \tag{8}$$

When introducing the Debye–Hückel parameter in equation (8), equation (9) is found to be

$$\rho_e = -\varepsilon\varepsilon_0\kappa^2\phi. \tag{9}$$

The boundary conditions of equation (6) for the conducting fluid are

$$y = 0 \qquad \phi = \zeta_1 \quad \text{for the bottom wall} \tag{10}$$

$$y = h_1 \qquad \phi = \zeta_2 \quad \text{for the interface.} \tag{11}$$

Equation (6) can be non-dimensionalized as

$$\frac{\mathrm{d}^2\phi^*}{\mathrm{d}y^{*2}} = K^2\phi^* \tag{12}$$

where

$$\phi^* = \frac{z_0 e\phi}{k_b T} \tag{13}$$

$$y^* = \frac{y}{h} \tag{14}$$

$$K = \kappa h. \tag{15}$$

The boundary conditions of equation (12) in a non-dimensional form can be written as

$$y^* = 0 \qquad \phi^* = \zeta_1^* \tag{16}$$

$$y^* = h_1^* \qquad \phi^* = \zeta_2^* \tag{17}$$

where

$$h_1^* = \frac{h_1}{h} \tag{18}$$

$$\zeta_1^* = \frac{z_0 e\zeta_1}{k_b T} \tag{19}$$

$$\zeta_2^* = \frac{z_0 e\zeta_2}{k_b T}. \tag{20}$$

The net charge density in a non-dimensional form is expressed as

$$\rho_e^* = \frac{\rho_e}{n_\infty z_0 e}. \tag{21}$$

When considering the expression of ϕ^*, equation (21) becomes

$$\rho_e^* = -2\phi^*. \tag{22}$$

When considering the boundary conditions, equations (16) and (17), the analytical solution of equation (12) can be written as

$$\phi^* = \frac{\zeta_2^*\sinh(Ky^*) - \zeta_1^*\sinh(Ky^* - Kh_1^*)}{\sinh(Kh_1^*)}. \tag{23}$$

When using equation (23), the net charge density, which is required to determine the electrostatic force caused by the presence of an EDL, can be given as

$$\rho_e^* = 2\frac{\zeta_1^*\sinh(Ky^* - Kh_1^*) - \zeta_2^*\sinh(Ky^*)}{\sinh(Kh_1^*)}. \tag{24}$$

3.2. Hydrodynamic field

For a one-dimensional steady fully-developed laminar flow through a microchannel between two parallel plates, as shown in figure 1, the pressure force is applied to an element of each fluid and the electric body force acts as a conducting fluid element. The electric body force is a result of the application of an external electric field. Taking these forces into account, the modified Navier–Stokes equation in x direction can be written for the conducting fluid as

$$0 = -\frac{\partial p}{\partial x} + \mu_1\frac{\partial^2 u_1}{\partial y^2} + E\rho_e \tag{25}$$

where $E\rho_e$ and E are the electric body force and the electric field, respectively. The value of E is assumed to be constant.

The pressure and the flow velocity depend only on x and y, respectively. The pressure gradient in x direction is assumed to be constant.

When assuming $P_x = -\frac{\mathrm{d}p}{\mathrm{d}x}$, equation (25) can be written as

$$0 = P_x + \mu_1 \frac{\mathrm{d}^2 u_1}{\mathrm{d}y^2} + E\rho_e. \tag{26}$$

When using the expression of ρ_e from equation (9), equation (26) becomes

$$0 = P_x + \mu_1 \frac{\mathrm{d}^2 u_1}{\mathrm{d}y^2} - \varepsilon\varepsilon_0\kappa^2 E\phi. \tag{27}$$

When dividing equation (27) by μ_1, equation (28) is found to be

$$0 = \frac{P_x}{\mu_1} + \frac{\mathrm{d}^2 u_1}{\mathrm{d}y^2} - \frac{\varepsilon\varepsilon_0\kappa^2 E}{\mu_1}\phi. \tag{28}$$

For the electric nonconducting fluid, the Navier–Stokes equation can be expressed as

$$0 = -\frac{\partial p}{\partial x} + \mu_2 \frac{\partial^2 u_2}{\partial y^2}. \tag{29}$$

When dividing equation (29) by μ_2, equation (29) can be written as

$$0 = \frac{P_x}{\mu_2} + \frac{\mathrm{d}^2 u_2}{\mathrm{d}y^2}. \tag{30}$$

Equations (28) and (30) are two second-order differential equations. Thus, four boundary conditions are required in order to solve them.

The no-slip boundary conditions can be expressed as

$$u_1(0) = 0 \tag{31}$$

$$u_2(h) = 0. \tag{32}$$

The same velocity at the interface between the two fluids is assumed to be

$$u_1(h_1) = u_2(h_1). \tag{33}$$

Furthermore, the shear stress is the same on the two fluids at the interface

$$\mu_1 \frac{\mathrm{d}u_1}{\mathrm{d}y}\bigg|_{y=h_1} = \mu_2 \frac{\mathrm{d}u_2}{\mathrm{d}y}\bigg|_{y=h_1}. \tag{34}$$

In a non-dimensional form, equation (28) is given as

$$0 = \frac{P_x}{\mu_1} + \frac{u_0}{h^2}\frac{\partial^2 u_1^*}{\partial y^{*2}} - \frac{\varepsilon\varepsilon_0\kappa^2 E}{\mu_1}\left(\frac{k_b T}{z_0 e}\phi^*\right) \tag{35}$$

with

$$u_1^* = \frac{u_1}{u_0} \tag{36}$$

where u_0 is an arbitrary reference velocity.

When dividing equation (35) by $\frac{u_0}{h^2}$ and introducing the Helmholtz–Smoluchowski electroosmotic velocity, $u_h = \frac{E\varepsilon\varepsilon_0 K_b T}{z_0 e \mu_1}$, equation (37) is found to be

$$0 = \frac{h^2 P_x}{\mu_1 u_0} + \frac{\mathrm{d}^2 u_1^*}{\mathrm{d}y^{*2}} - \frac{u_h \kappa^2 h^2}{u_0}\phi^*. \tag{37}$$

After arranging equation (37) and introducing K, equation (38) is obtained as follows:

$$0 = \frac{h^2 P_x}{\mu_1 u_0} + \frac{\mathrm{d}^2 u_1^*}{\mathrm{d}y^{*2}} - \frac{u_h}{u_0}K^2\phi^*. \tag{38}$$

After simplifying equation (38), it becomes

$$0 = C_0 + \frac{\mathrm{d}^2 u_1^*}{\mathrm{d}y^{*2}} - C_1 K^2 \phi^* \tag{39}$$

where $C_0 = \frac{h^2 P_x}{\mu_1 u_0}$ and $C_1 = \frac{u_h}{u_0}$.

When taking equation (12) into account, equation (39) can be expressed as

$$0 = C_0 + \frac{\mathrm{d}^2 u_1^*}{\mathrm{d}y^{*2}} - C_1 \frac{\mathrm{d}^2 \phi^*}{\mathrm{d}y^{*2}}. \tag{40}$$

When integrating equation (40) twice, equation (41) is found to be

$$\frac{C_0 y^{*2}}{2} + u_1^* - C_1\phi^* = a_1 y^* + a_2. \tag{41}$$

The constants of integration, a_1 and a_2, can be determined using the boundary conditions, equations (31)–(34), in a non-dimensional form.

From equation (41), the flow velocity of fluid 1 can be written as

$$u_1^* = -\frac{C_0 y^{*2}}{2} + C_1\phi^* + a_1 y^* + a_2. \tag{42}$$

For fluid 2, equation (30) can be expressed in a non-dimensional form as

$$0 = \frac{P_x}{\mu_2} + \frac{u_0}{h^2}\frac{\mathrm{d}^2 u_2^*}{\mathrm{d}y^{*2}} \tag{43}$$

with

$$u_2^* = \frac{u_2}{u_0}. \tag{44}$$

When dividing equation (43) by $\frac{u_0}{h^2}$, equation (45) is obtained as follows:

$$0 = \frac{h^2 P_x}{\mu_2 u_0} + \frac{\mathrm{d}^2 u_2^*}{\mathrm{d}y^{*2}}. \tag{45}$$

When introducing the constant $C_2 = \frac{h^2 P_x}{\mu_2 u_0}$, equation (45) becomes

$$0 = C_2 + \frac{\mathrm{d}^2 u_2^*}{\mathrm{d}y^{*2}}. \tag{46}$$

When integrating equation (46) twice, equation (47) is found to be

$$\frac{C_2 y^{*2}}{2} + u_2^* = b_1 y^* + b_2 \tag{47}$$

where b_1 and b_2 are the integration constants to be determined from the boundary conditions, equations (31)–(34), in a non-dimensional form.

Finally, from equation (47), the flow velocity for fluid 2 can be expressed as

$$u_2^* = -\frac{C_2 y^{*2}}{2} + b_1 y^* + b_2. \tag{48}$$

When applying the boundary conditions in a non-dimensional form for equations (42) and (48):

For the no-slip boundary condition for fluid 1,

$$u_1^*(y^* = 0) = 0. \tag{49}$$

From equation (42), equation (50) is found to be

$$u_1^*(0) = a_2 + C_1\zeta_1^* = 0. \tag{50}$$

From equation (50), a_2 can be written as

$$a_2 = -C_1\zeta_1^*. \tag{51}$$

For fluid 2, the no-slip boundary condition in a non-dimensional form can be expressed as

$$u_2^*(y^* = 1) = 0. \tag{52}$$

From equation (48), equation (53) is obtained as follows:

$$u_2^*(1) = -\frac{C_2}{2} + b_1 + b_2 = 0. \tag{53}$$

From equation (53), b_2 can be determined as

$$b_2 = \frac{C_2}{2} - b_1. \tag{54}$$

The boundary condition in a non-dimensional form concerning the same flow velocity at the interface between the two fluids is given as

$$u_1^*(h_1^*) = u_2^*(h_1^*). \tag{55}$$

When using equations (42) and (48), equation (56) is found to be

$$-\frac{C_0}{2}h_1^{*2} + a_1 h_1^* + C_1\zeta_2 + a_2 = -\frac{C_2}{2}h_1^{*2} + b_1 h_1^* + b_2. \tag{56}$$

After transforming equation (56), it can be written as

$$a_1 h_1^* + a_2 - b_1 h_1^* - b_2 - \frac{C_0}{2}h_1^{*2} + \frac{C_2}{2}h_1^{*2} + C_1\zeta_2 = 0. \tag{57}$$

From equation (34), the boundary condition in a non-dimensional form for the same shear stress on the two fluids at the interface can be written as

$$\mu_1 \frac{u_0}{h}\frac{\mathrm{d}u_1^*}{\mathrm{d}y^*}\bigg|_{y^*=h_1^*} = \mu_2 \frac{u_0}{h}\frac{\mathrm{d}u_2^*}{\mathrm{d}y^*}\bigg|_{y^*=h_1^*}. \tag{58}$$

When introducing the dynamic viscosity ratio $\alpha = \frac{\mu_2}{\mu_1}$, equation (58) becomes

$$\frac{\mathrm{d}u_1^*}{\mathrm{d}y^*}\bigg|_{y^*=h_1^*} = \alpha \frac{\mathrm{d}u_2^*}{\mathrm{d}y^*}\bigg|_{y^*=h_1^*}. \tag{59}$$

The partial differential of u_1^* in y^* direction can be given as

$$\tau_1^* = \frac{\mathrm{d}u_1^*}{\mathrm{d}y^*} = -C_0 y^* + a_1 + \frac{KC_1}{\sinh(Kh_1^*)}(\zeta_2^* \cosh(Ky^*) - \zeta_1^* \cosh(Ky^* - Kh_1^*)) \tag{60}$$

where τ_1^* is defined as the non-dimensional shear stress for fluid 1.

For fluid 2, the partial differential of u_2^* in y^* direction can be expressed as

$$\frac{\mathrm{d}u_2^*}{\mathrm{d}y^*} = -C_2 y^* + b_1 \tag{61}$$

where $\tau_2^* = \alpha\frac{\mathrm{d}u_2^*}{\mathrm{d}y^*}$ is the non-dimensional shear stress for fluid 2.

When substituting equations (60) and (61) into equation (59), equation (62) is found to be

$$-C_0 h_1^* + \frac{KC_1}{\sinh(Kh_1^*)}(\zeta_2^* \cosh(Kh_1^*) - \zeta_1^*) + a_1 = -\alpha C_2 h_1^* + \alpha b_1. \tag{62}$$

After arranging equation (62), it can be written as

$$a_1 - \alpha b_1 - C_0 h_1^* + \alpha C_2 h_1^* + \frac{KC_1}{\sinh(Kh_1^*)} \times (\zeta_2^* \cosh(Kh_1^*) - \zeta_1^*) = 0. \tag{63}$$

From equation (63), a_1 is given as

$$a_1 = \alpha b_1 + C_0 h_1^* - \alpha C_2 h_1^* - \frac{KC_0}{\sinh(Kh_1^*)}(\zeta_2^* \cosh(Kh_1^*) - \zeta_1^*). \tag{64}$$

When substituting equations (51), (54) and (64) into equation (57), equation (65) is obtained as follows:

$$\alpha b_1 h_1^* + C_0 h_1^{*2} - \alpha C_2 h_1^{*2} - \frac{KC_1}{\sinh(Kh_1^*)}h_1^* \times (\zeta_2^* \cosh(Kh_1^*) - \zeta_1^*) - C_1\zeta_1^* - b_1 h_1^* - \left(\frac{C_2}{2} - b_1\right) - \frac{C_0}{2}h_1^{*2} + \frac{C_2}{2}h_1^{*2} + C_1\zeta_2^* = 0. \tag{65}$$

After transforming equation (65), it becomes

$$\alpha b_1 h_1^* - b_1 h_1^* + b_1 = -C_0 h_1^{*2} + \alpha C_2 h_1^{*2} + \frac{KC_1}{\sinh(Kh_1^*)}h_1^* \times (\zeta_2^* \cosh(Kh_1^*) - \zeta_1^*) + C_1\zeta_1^* + \frac{C_2}{2} + \frac{C_0}{2}h_1^{*2} - \frac{C_2}{2}h_1^{*2} - C_1\zeta_2^*. \tag{66}$$

From equation (66), b_1 can be expressed as

$$b_1 = \frac{1}{h_1^*(\alpha - 1) + 1}\left(h_1^{*2}\left(-\frac{C_0}{2} - \frac{C_2}{2}\right) + \alpha C_2 h_1^{*2} + \frac{C_2}{2} + \frac{KC_1}{\sinh(Kh_1^*)}h_1^*(\zeta_2^* \cosh(Kh_1^*) - \zeta_1^*) + C_1(\zeta_1^* - \zeta_2^*)\right). \tag{67}$$

After determining b_1 using equation (67), the constants a_1, a_2 and b_2 are calculated using equations (51), (54) and (64).

3.3. Non-dimensional volumetric flow rates

The volumetric flow rate between the parallel plates is determined by integrating the flow velocity distribution over the cross-sectional area. For fluid 1, the non-dimensional volumetric flow rate is defined as follows:

$$Q_1^* = \int_0^{h_1^*} u_1^* \,\mathrm{d}y^*. \tag{68}$$

When substituting equation (42) into equation (68) and integrating equation (68), Q_1^* can be expressed as

$$Q_1^* = -\frac{C_0}{6}h_1^{*3} + \frac{a_1}{2}h_1^{*2} + a_2 h_1^* + \frac{C_1}{K\sinh(Kh_1^*)} \times (\zeta_2^*(\cosh(Kh_1^*) - 1) - \zeta_1^*(1 - \cosh(Kh_1^*))). \tag{69}$$

For fluid 2, the dimensionless volumetric flow rate is given as

$$Q_2^* = \int_{h_1^*}^{1} u_2^* \,\mathrm{d}y^*. \tag{70}$$

When substituting equation (48) into equation (70) and integrating equation (70), Q_2^* is given as

$$Q_2^* = -\frac{C_2}{6}\left(1 - h_1^{*3}\right) + \frac{b_1}{2}\left(1 - h_1^{*2}\right) + b_2(1 - h_1^*). \tag{71}$$

The non-dimensional means flow velocities can be defined from equations (70) and (71). For fluid 1, the means flow velocity, $\bar{u}_1^*$, can be written as

$$\bar{u}_1^* = \frac{Q_1^*}{h_1^*}, \tag{72}$$

and, for fluid 2, the means flow velocity, $\bar{u}_2^*$, is given as

$$\bar{u}_2^* = \frac{Q_2^*}{h_2^*}. \tag{73}$$

Table 1. Constant data used for the simulations.

ε_0 (C m^{-1} V^{-1})	ε	n_∞ (m^{-3})	z_0	E (V m^{-1})	L (m)	h (m)	h_1 (m)	u_0 (m s^{-1})
8.854×10^{-12}	80	6.022×10^{-20}	1	5×10^4	0.02	35×10^{-6}	17×10^{-6}	1

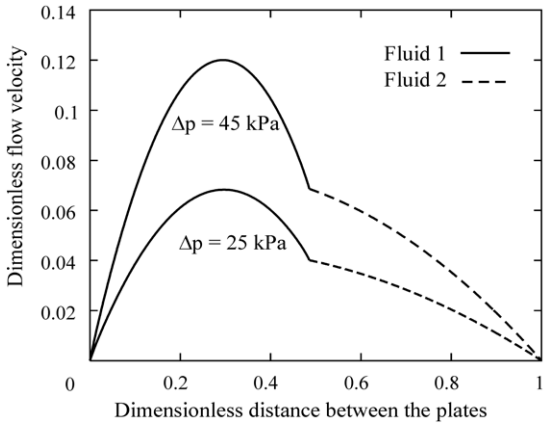

Figure 2. Dimensionless flow velocity versus dimensionless distance between the plates (parameter: pressure difference).

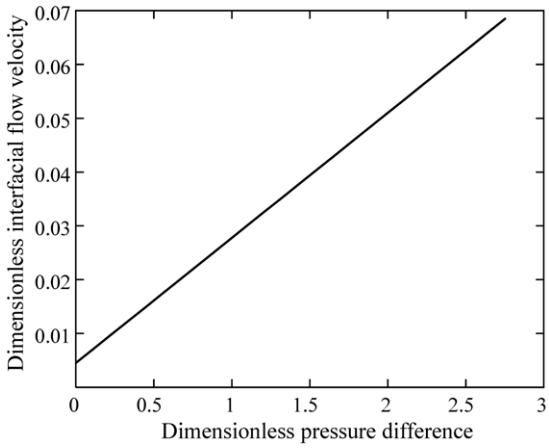

Figure 3. Dimensionless interfacial flow velocity versus dimensionless pressure difference.

4. Numerical results and discussion

From the equations found in section 3, a FORTRAN program was written to numerically investigate and analyze the effects of the pressure difference, the interface position, the interfacial zeta potential, the dynamic viscosity ratio and the zeta potential on the flow characteristics of the two fluids in a microchannel between two plates. For the achieved simulations, table 1 gives the used constant data for the permittivity of the vacuum, the dimensionless dielectric constant, the ionic number concentration in the bulk solution, the valence of ions, the electric field, the plate length, the plate height, the interface position and the reference velocity.

4.1. Effect of pressure difference

To examine the effect of the pressure difference in a microchannel on the flow velocity, the dynamic viscosity ratio, the wall zeta potential, the interfacial zeta potential and the interface position were kept constant with the values of 10, -0.024 V, -0.024 V and 17 μm, respectively. The pressure differences of 25 kPa and 45 kPa were chosen. Figure 2 shows the flow velocity distribution in the microchannel cross-section. There, it can be observed that the flow velocities for both fluids increase when the pressure difference between the microchannel inlet and outlet increases. The maximal value of the flow velocity for fluid 1 is greater than that for fluid 2. The curve of the interfacial flow velocity for both fluids as a function of the pressure difference is shown in figure 3, where it can be observed that the interfacial flow velocity increases with the pressure difference. For the volumetric flow velocity, it can be observed in figure 4 that the volumetric flow velocity increases when the pressure difference increases. The volumetric flow rate for fluid 1 is greater than that for fluid 2.

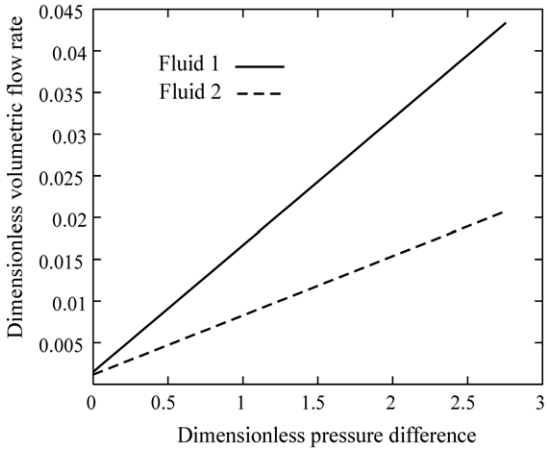

Figure 4. Dimensionless volumetric flow rate versus dimensionless pressure difference.

4.2. Effect of the interface position

To examine the effect of the interface position on the volumetric flow rate, the interfacial flow velocity and the interfacial shear stress; the dynamic viscosity ratio, the wall zeta potential, the interfacial zeta potential and the pressure difference were kept constant with the values of 10, -0.024 V, -0.024 V and 45 kPa, respectively. The interface position of both fluids was varied from 8 μm to 19.25 μm. Figure 5 shows the volumetric flow rate as a function of the interface position. There, it can be remarked that the volumetric flow rate of fluid 1 increases when the interface position increases, while that for fluid 2 decreases when the interface position increases. The curve of the interfacial flow velocity for both fluids as a function of the interface position is shown in figure 6, where it can be observed that the interfacial velocity decreases when the interface position increases. In figure 7, the interfacial

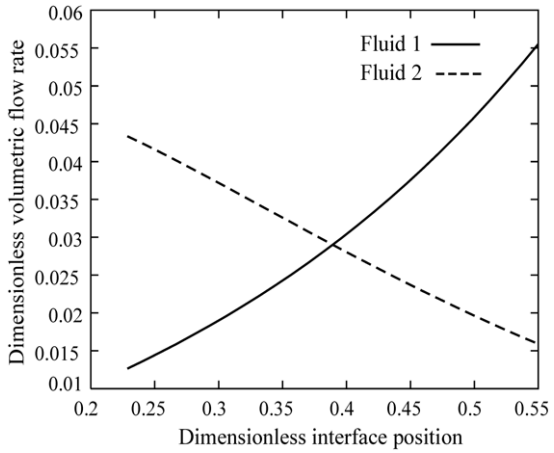

Figure 5. Dimensionless volumetric flow rate versus dimensionless interface position.

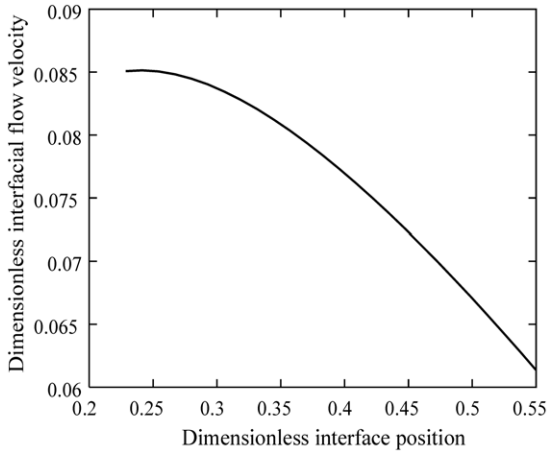

Figure 6. Dimensionless interfacial flow velocity versus dimensionless interface position.

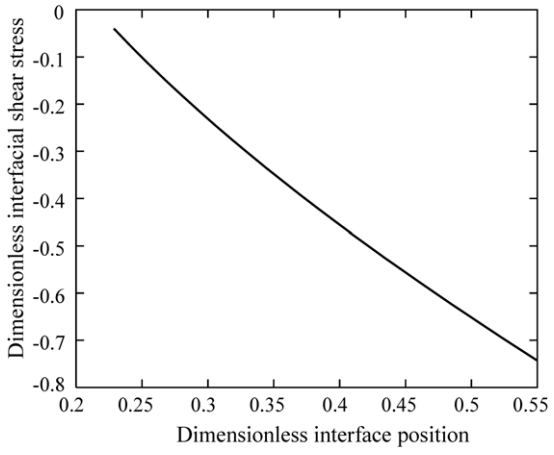

Figure 7. Dimensionless shear stress versus dimensionless interface position.

shear stress for both fluids is presented as a function of the interface position. There, it can be seen that the absolute value of the interfacial shear stress increases when the interfacial position increases.

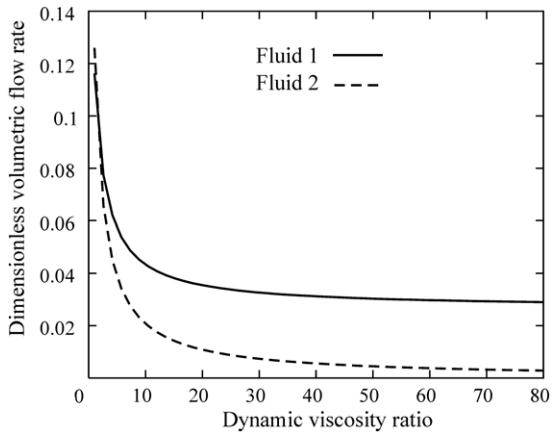

Figure 8. Dimensionless volumetric flow rate versus dynamic viscosity ratio.

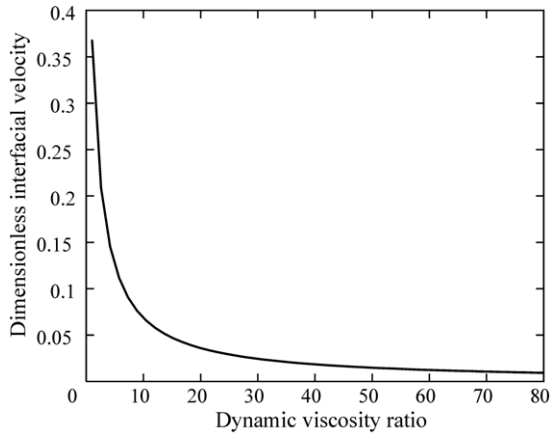

Figure 9. Dimensionless interfacial velocity versus dynamic viscosity ratio.

4.3. Effect of dynamic viscosity ratio

To analyze the effect of the dynamic viscosity ratio between both fluids on the volumetric flow rate, the interfacial flow velocity and the flow velocity distribution; the wall zeta potential, the interfacial zeta potential, the pressure difference and the interface position were kept constant with the values of -0.024 V, -0.024 V, 45 kPa and 17 μm. The dynamic viscosity ratio was varied from 1 to 80. Figure 8 represents the volumetric flow rate as a function of the dynamic viscosity ratio. From this figure, it can be observed that the volumetric flow rate decreases when the dynamic viscosity ratio for both fluids increases. The volumetric flow rate for fluid 1 was greater than that for fluid 2. The curve of the interfacial velocity as a function of the dynamic viscosity ratio was shown in figure 9. There, it can be observed that the interfacial velocity was strongly dependent on the dynamic viscosity ratio. Figure 10 demonstrates the distribution of the flow velocity for both fluids as a function of the distance between the plates, when the values of 1, 10 and 20 for the dynamic velocity ratio are considered. From this figure, it can be observed that the optimum of the flow velocity for both fluids decreases when the dynamic viscosity ratio increases. The maximum flow velocity for fluid 1 was higher than that for fluid 2.

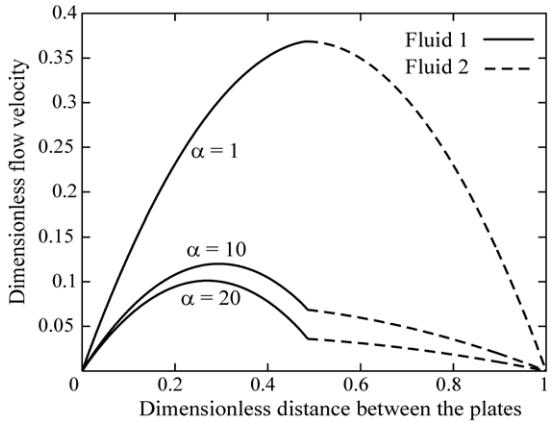

Figure 10. Dimensionless flow velocity versus dimensionless distance between the plates (parameter: dynamic viscosity ratio).

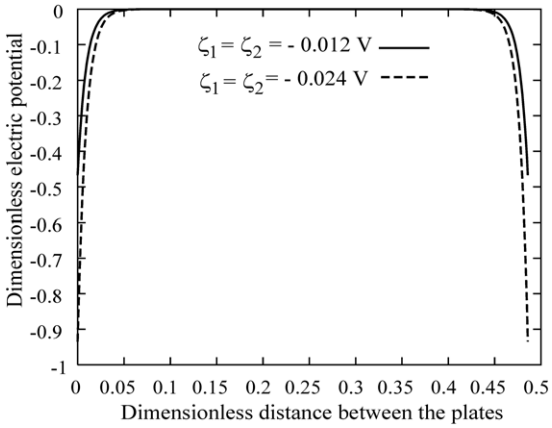

Figure 11. Dimensionless electric potential versus dimensionless distance between the plates (parameter: zeta potential).

4.4. Effect of zeta potential

To examine the effect of the zeta potential on the electric potential, the electric potential was represented as a function of the distance between the plates for two different values of the zeta potentials. Figure 11 demonstrates the influence of the variation of the zeta potential on the electric potential assuming the same value for the wall zeta potential and the interfacial zeta potential. From this figure, it can be observed that the effect of the zeta potential is focused on the microchannel bottom wall of fluid 1 and the interface position of both fluids.

4.5. Model comparison

To validate the developed mathematical model, the results obtained for the flow velocity of the conducting fluid were compared with those achieved using the analytical approach described in [4] for a single conducting fluid flow through a parallel plates microchannel. In this results comparison, the chosen values of 45 kPa, −0.024 V, 50 000 V m^{-1}, 0.001 Pa s and 25 μm were used for the difference pressure, the zeta potential, the electric field, the dynamic viscosity and the distance between the plates, respectively. Figure 12 represents the variation of the flow velocity of the conducting fluid as a function of the microchannel height. There, it can be observed that the results from the analytical approach described in [4] and the results from the present work concur.

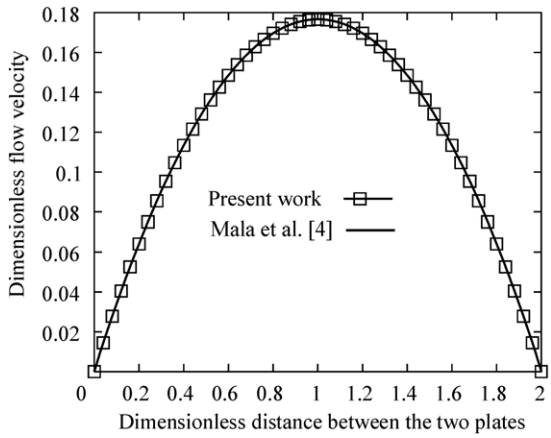

Figure 12. Comparison of dimensionless flow velocity between the present work and the study of Mala *et al* [4].

5. Conclusion

In this study, a mathematical model of the flow of two immiscible fluids in a microchannel between two parallel plates was developed and analyzed while taking into consideration the concept of pumping an electric nonconducting fluid using an electric conducting fluid. Based on the Poisson–Boltzmann and modified Navier–Stokes equations, the expressions of the electric potential, the flow velocity, the volumetric flow rate and the interfacial shear stress were found by taking into account the combined effect of the pressure gradient and electroosmosis. The results obtained demonstrate that the variation of the interface position, the dynamic viscosity ratio, the zeta potentials and the pressure difference affects the static flow behavior in a microchannel in a strong yet different manner. Furthermore, the results demonstrate the interfacial shear stress tendency to decrease when the interface position increases. The developed model demonstrates the concurrence with the results obtained using an analytical approach for a single conducting fluid, as described in [4].

Acknowledgment

The authors are grateful to the Institutional Fund of Research of the University of Quebec (FIR).

References

[1] Nguyen N-T and Wereley S T 2002 *Fundamentals and Applications of Microfluidics* (Boston, MA: Artech House Publishers)

[2] Zeng S, Chen C-H, Mikkelsen J C Jr and Santiago J G 2001 Fabrication and characterization of electroosmotic micropumps *Sensors Actuators* B **79** 107–14

[3] Brask A, Goranovic G, Jensen M J and Bruus H 2005 A novel electro-osmotic pump design for nonconducting liquids: theoretical analysis of flow rate–pressure characteristics and stability *J. Micromech. Microeng.* **15** 883–91

[4] Mala Gh M, Li D, Werner C, Jacobasch H-J and Ning Y B 1997 Flow characteristics of water through a microchannel between two parallel plates with electrokinetic effects *Int. J. Heat Fluid Flow* **18** 489–96
[5] Patankar N A and Hu H H 1998 Numerical simulation of electroosmotic flow *Anal. Chem.* **70** 1870–81
[6] Vainshtein P and Gutfinger C 2002 On electroviscous effects in microchannels *J. Micromech. Microeng.* **12** 252–6
[7] Yang R-J, Fu L-M and Lin Y-C 2001 Electroosmotic flow in microchannels *J. Colloid Interface Sci.* **239** 98–105
[8] Gao Y, Wong T N, Yang C and Ooi K T 2005 Two-fluid electroosmotic flow in microchannels *J. Colloid Interface Sci.* **284** 306–14
[9] Chan W K and Yang C 2005 Surface-tension-driven liquid-liquid, displacement in a capillary *J. Micromech. Microeng.* **15** 1722–8